

# Experimental Study on the Thermal Performance of a Small-scale Loop Heat Pipe with Polypropylene Wick

Joon Hong Boo\*, Won Bok Chung

*School of Aerospace and Mechanical Engineering, Hankuk Aviation University, 200-1, Hwajeon-dong, Deogyang-gu, Goyang-city, Gyeonggi-do 412-791, Korea*

A small-scale loop heat pipe (LHP) with polypropylene wick was fabricated and tested for investigation of its thermal performance. The container and tubing of the system were made of stainless steel and several working fluids were tested including methanol, ethanol, and acetone. The heating area was 35 mm × 35 mm and nine axial grooves were provided in the evaporator to provide vapor passages. The pore size of the polypropylene wick inside the evaporator was varied from 0.5 μm to 25 μm. The inner diameter of liquid and vapor transport lines were 2.0 mm and 4.0 mm, respectively and the length of which were 0.5 m. The size of condenser was 40 mm (W) × 50 mm (L) in which ten coolant paths were provided. Start-up characteristics as well as steady-state performance was analyzed and discussed. The minimum thermal load of 10 W (0.8 W/cm<sup>2</sup>) and maximum thermal load of 80 W (6.5 W/cm<sup>2</sup>) were achieved using methanol as working fluid with the condenser temperature of 20°C with horizontal position.

**Key Words :** Loop Heat Pipe, Polypropylene Wick, Heat Transport Limit, Start-up Characteristics

## Nomenclature

$d$  : Differential or derivative  
 $g$  : Gravity acceleration (m/s<sup>2</sup>)  
 $h_{fg}$  : Latent heat of vaporization (J/kg)  
 $K$  : Permeability (m<sup>2</sup>)  
 $L_t$  : Liquid transport length (m)  
 $m$  : Mass of the fluid charge (kg)  
 $P$  : Pressure (Pa)  
 $Q_{in}$  : Input thermal load (W)  
 $R_{th}$  : Thermal resistance (K/W)  
 $r_{cap}$  : Effective capillary radius (m)  
 $T$  : Temperature (°C)  
 $T_{cool,in}$  : Inlet temperature of the coolant (°C)  
 $V$  : Volume (m<sup>3</sup>)  
 $\bar{v}_t$  : Apparent liquid velocity through porous medium (m/s)

## Greek symbols

$\phi$  : Volume ratio of liquid in the reservoir to reservoir  
 $\mu$  : Viscosity  
 $\rho$  : Density (kg/m<sup>3</sup>)  
 $\sigma$  : Surface tension (N/m)

## Subscripts

$c$  : Condenser  
 $cap$  : Capillary  
 $e$  : Evaporator  
 $g$  : Groove  
 $H$  : Heater  
 $l$  : Liquid  
 $p$  : Transport line  
 $r$  : Reservoir  
 $sat$  : Saturated state  
 $v$  : Vapor  
 $w$  : Wick

\* Corresponding Author,

E-mail : jhboo@hau.ac.kr

TEL : +82-2-300-0107; FAX : +82-2-3158-2191

School of Aerospace and Mechanical Engineering, Hankuk Aviation University, 200-1, Hwajeon-dong, Deogyang-gu, Goyang-city, Gyeonggi-do 412-791, Korea. (Manuscript Received November 5, 2004; Revised February 25, 2005)

## 1. Introduction

The loop heat pipe (hereinafter denoted by

LHP) was developed in the early 1970s and was actively employed as thermal control devices since early 1980s especially in aerospace applications (Kiseev et al., 1984 ; Maidanik et al., 1985). The basic operating principle of LHP is similar to a conventional heat pipe in that they utilize the phase change of working fluid while the working fluid circulates between evaporator and condenser. In LHP, however, the evaporator and condenser are physically separated and connected with separate liquid and vapor lines, of which the diameters are usually much smaller than that of conventional heat pipes (See Fig. 1). Furthermore, the wick structure is confined within the evaporator to reduce the pressure drops for the flow through liquid and vapor lines. A liquid-saturated porous wick in LHP evaporator is placed in contact with a heat transfer surface, where escaping passages (usually in grooved shape) for generated vapor are provided. LHP is distinguished from the capillary pumped loop (CPL) by an embedded liquid reservoir, which is installed as a separate container in the latter. As a result of the configuration change from a conventional heat pipe, LHP is typically characterized by higher thermal heat transport capability and enhanced performance against gravity. The performance of the LHP makes the most attractive thermal control device for space applications (Goncharov et al., 1995 ; Kozmine et al., 1996; Schlitt, R., 2000, Ishikawa et al., 2001 ; Hoang and Ku, 2002 ; Swanson et al., 2003).

Most LHPs in previous studies were made of sintered metal powder (usually nickel or titanium) of 0.3  $\mu\text{m}$  to 5  $\mu\text{m}$  pore size as a capillary

structure and ammonia as a working fluid. In addition, the evaporators have been made in cylindrical shape and the operating temperature range was usually from  $-20$  to  $100^\circ\text{C}$  (Maidanik, 1999). However, the use of LHP in commercial and terrestrial applications has been limited due to a high manufacturing cost of the wick material and relative difficulty in design and fabrication of the system.

Quite a few studies have been conducted recently to apply LHP to thermal control of electronic devices and equipments for terrestrial applications by adopting various geometries, working fluids, and wick structures. Boo et al.(1995) demonstrated a successful operation of a LHP using a flat evaporator where coarse screen mesh was employed for the first time as an alternative means of vapor passages. Bienert et al.(1999) fabricated and tested a small LHP of which the system size was 229 mm by 127 mm and transported thermal load of 50 W at the operating temperature of  $50^\circ\text{C}$ . Pastukhov et al.(1999) tested LHP in which the diameter of the transport line was 1 mm and 40 W thermal load was able to be transported up to 0.5 m at the operating temperature of  $70^\circ\text{C}$ . Boo (2000) fabricated and tested CPL without reservoir (LHP) using ethanol as working fluid and ceramic fiber wick as a capillary structure. The LHP had a flat type evaporator, 200 mm by 100 mm, and screen mesh was used as vapor passages. The maximum heat flux of about  $5 \text{ W/cm}^2$  was achieved. Delil et al. (2002) reported development of a LHP having a flat disk-type evaporator. The maximum thermal load was 120 W and the thermal resistance was about 0.6 K/W using ethanol-nickel compositions. Bazzo et al.(2002) studied a capillary pumping system to assist flat solar collectors using acetone as a working fluid. The heat load capacity of approximately  $0.5 \text{ W/cm}^2$  was achieved in their study. Kobayashi et al.(2003) fabricated and tested a LHP using R134a as a working fluid and Teflon as a wick material of the capillary pumping evaporator which transported 135 W at horizontal position. Lee at al. (2004) was tried distilled water as a working fluid of a sintered brass power wick LHP having

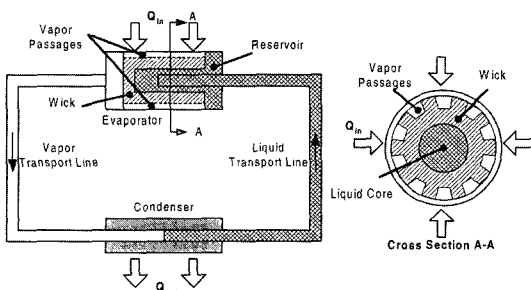


Fig. 1 Typical LHP operation (schematic)

flat type evaporator. The maximum thermal loads was 70 W ( $2.8 \text{ W/cm}^2$ ) and the thermal resistance was about 1 K/W.

In this study, a small-scale loop heat pipe was fabricated and tested to employ a low-cost wick structure and easily manageable working fluids which may alleviate the shortcomings of existing LHP for certain applications. Polypropylene (hereinafter denoted by PP) wick was selected as capillary structure of LHP. PP is known to be chemically stable with most of low temperature working fluids such as water, alcohol, and acetone. The typical limitation of PP wick can be met in the operating temperature. Specification of the wick is summarized in Table 1, where the 'operating limit' means an allowable temperature at which its shape is not deformed (Waterman and Ashby, 1997). PP wick LHPs were manufactured with working fluids for low temperature range application. The LHP in this study had a flat surface evaporator for easiness in electronics cooling applications. The performance of LHP was observed from the view points of pore size of capillary structure, working fluids and their charge ratios, and condenser temperature.

**Table 1** Specification of polypropylene wick

Material	Polypropylene, PP	
Pore Size	0.5~25 $\mu\text{m}$	
Porosity	0.4~0.5	
Melting Temperature	1 bar	160~170°C
Operating Limit	4.5 bar	90~120°C
	18 bar	48~65°C
Thermal Conductivity	0.2 W/mK	

## 2. Experimental Setup

The LHP was composed of a flat type evaporator with reservoir, vapor and liquid transport lines, and a condenser as shown in Fig. 2. The outer dimension of the evaporator was 40 mm (W)  $\times$  50 mm (L)  $\times$  30 mm (H), with an embedded reservoir. The heating area in the evaporator was 35 mm  $\times$  35 mm and where nine axial grooves were provided to serve as vapor passage. PP wick of 5 mm thickness was in contact with axial grooves tightly by a compression spring. The condenser was 40 mm (W)  $\times$  50 mm (L) in which ten coolant paths were provided. The inner diameter of liquid and vapor transport lines were 2.0 mm and 4.0 mm, respectively and the length of which were 0.5 m. The heating block was made of aluminum and three electric cartridge heaters. Four T-type thermocouples, AWG 30 (wire O.D. of 0.25 mm, max. error 0.5°C) were inserted inside of the vapor and liquid lines at its ends and other thermocouples were attached to the wall of each part as shown in the Fig. 2. Five T-type thermocouples were attached to the surface of the heating block to measure the average temperature. Thermal compound was applied between the evaporator and the heating block. The whole LHP was insulated with ceramic wool.

The LHP was installed on a test bench so that the tilt angle can be adjusted during the test. The thermal load was controlled by a voltage regulator and measured by a watt meter (max. error 0.5% F.S.). The temperature and flow rate of the coolant was controlled by an isothermal bath.

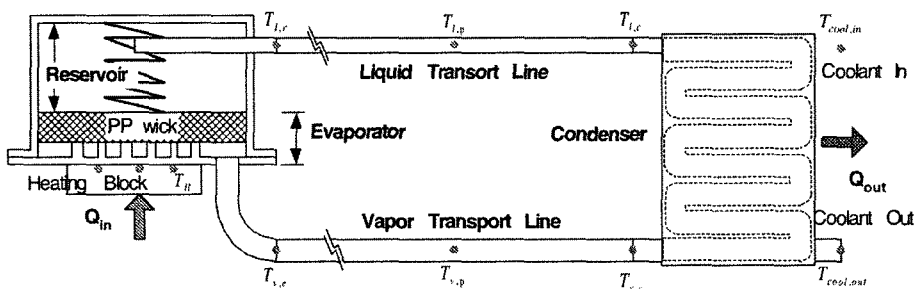


**Fig. 2** Schematic of PP wick LHP in this study with thermocouple locations (plane view)

During the experiment, the coolant flow rate was maintained 5 cc/s. The temperature data were acquired by a data acquisition system in every 2 seconds.

Performance test of the LHP was conducted for various conditions. The pore sizes of the PP wick used were 0.5, 1, 20 and 25  $\mu\text{m}$ . The nominal pore size of the wick in this study means that 93% of the particles of the designated size cannot pass through the wick. The thickness of the pore wick was 5 mm in all cases. Methanol, acetone, and ethanol were considered as suitable working fluids for PP wick LHP in this study. Working fluid charge is determined by the Eq (1). The fluid charge ratio is denoted by  $\phi$ , which varied from 0.1 to 0.7 during the experiment.

$$m_{\text{charge}} = \rho_l (\phi V_r + V_{l,p} + V_{v,p} + V_c + V_w + V_g) + \rho_v [(1-\phi) V_r] \quad (1)$$

Each performance test was conducted until the temperature of heater surface reached 90°C to protect the PP wick from permanent deformation. For this reason, the maximum thermal load is determined at this temperature. The minimum thermal load was determined when the vapor temperature at the evaporator outlet ( $T_{v,e}$ ) and the vapor temperature at the condenser inlet ( $T_{v,c}$ ) became identical within 1°C difference. Also, thermal resistance of the system was introduced to evaluate the thermal performance as in the following :

$$R_{th} [\text{K/W}] = \frac{T_H - T_{cool,in}}{Q_{in}} \quad (2)$$

where  $T_H$  is the average temperature of the heating block surface and  $T_{cool,in}$  is the coolant temperature supplied to the heat sink, and  $Q_{in}$  is thermal load supplied to the evaporator.

### 3. Results and Discussion

Figure 3 shows the steady-state temperature distribution as a function of thermal loads for methanol-0.5  $\mu\text{m}$  LHP for  $\phi=0.5$  and coolant temperature of 20°C ( $T_{cool,in}$  in Fig. 2). The heater surface was heated up to 55°C when 5 W thermal load was applied. While the temperature

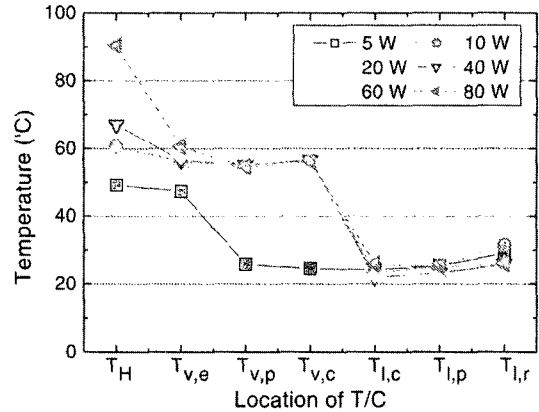


Fig. 3 Steady-state temperature distribution of methanol-0.5  $\mu\text{m}$  LHP for  $\phi=0.5$ ,  $T_{cool,in}=20^\circ\text{C}$

difference between heater ( $T_H$ ) and vapor at the evaporator outlet ( $T_{v,e}$ ) was only 2°C, the temperature at the outer wall in the middle of the vapor transport line ( $T_{v,p}$ ) and the condenser inlet ( $T_{v,c}$ ) were 25°C, and 24°C, and the temperature at the liquid inlet of the reservoir was 30°C. Based on this observation, the LHP did not start up at this condition. When thermal load of 10 W or higher was supplied, there were no temperature difference between  $T_{v,e}$  and  $T_{v,c}$ . It was observed that the working fluid was circulated normally. During thermal load was varied from 10 W to 80 W,  $T_H$  increased by 29°C (from 61°C to 90°C) while  $T_{v,e}$  increased only by 5°C (from 56°C to 61°C). It may be stated that the magnitude of thermal load between 10 and 80 W had only little influence on the operating temperature of the LHP. Similar results were observed for the other wick pore sizes, both in the distribution of steady-state temperature and in the weak dependency of operating temperature on the thermal load. The maximum thermal load was 80 W for methanol-0.5  $\mu\text{m}$  LHP and 20°C coolant temperature.

Figure 4 shows the effect of the wick pore size on the maximum thermal load and thermal resistance. The figure summarizes the results from four different pore sizes, which were 0.5, 1.0, 20, and 25  $\mu\text{m}$ . Among these cases the best performance was observed for the pore size of 0.5  $\mu\text{m}$ . As pore size reduced from 25  $\mu\text{m}$  to 0.5  $\mu\text{m}$ , the maximum

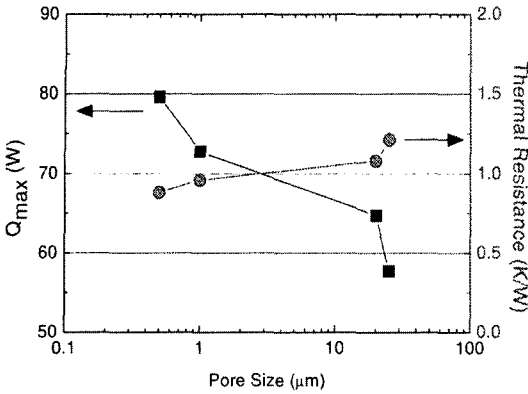


Fig. 4  $Q_{max}$  and  $R_{th}$  for pore size of PP wick (methanol LHP for  $\phi=0.5$ ,  $T_{cool,in}=20^{\circ}C$ )

thermal load was increased by 45%. At the same time, thermal resistance of the system was decreased by 33%. The pressure balance for operation of a LHP can be expressed as in the following equation (Maidanik et al., 1994).

$$\Delta P_{cap} = \frac{2\sigma}{r_{cap}} \geq \Delta P_{v,p} + \Delta P_{l,p} + \Delta P_w + \Delta P_{gravity} \quad (3)$$

In Eq. (3),  $\Delta P_{cap}$  denotes capillary pumping pressure which is the driving force of working fluid circulation through the loop and determined by the effective capillary radius ( $r_{cap}$ ).  $\Delta P_{v,p}$  and  $\Delta P_{l,p}$  are pressure drops associated with fluid flows in the vapor and liquid transport lines, respectively.  $\Delta P_w$  is pressure drop of the liquid flow through the wick which can be estimated by  $\mu_l \bar{v}_l L_l / K$ , where  $K$  is permeability of wick, and  $\Delta P_{gravity}$  is gravity head.  $\Delta P_{cap}$  increases linearly as pore size ( $r_{cap}$ ) reduces. And as  $\Delta P_{cap}$  becomes larger than the other terms on the right side of Eq. (3), the more working fluid can circulate the loop per unit time resulting in the enhancement of thermal performance of LHP.  $\Delta P_w$  is also affected by the size of  $r_{cap}$  since it involves permeability ( $K$ ), which normally decreases as the wick pore size reduces. Due to nonlinear relation with  $r_{cap}$ , permeability is usually determined by empirical methods. As  $r_{cap}$  reduced therefore, both  $\Delta P_{cap}$  and  $\Delta P_w$  should have been increased. In the LHP in this study however, it is considered that the gain in  $\Delta P_{cap}$  was larger than that in  $\Delta P_w$  and resulted in the net enhancement of thermal performance, which was

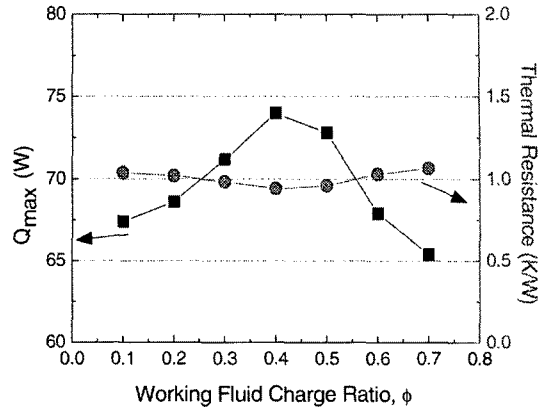
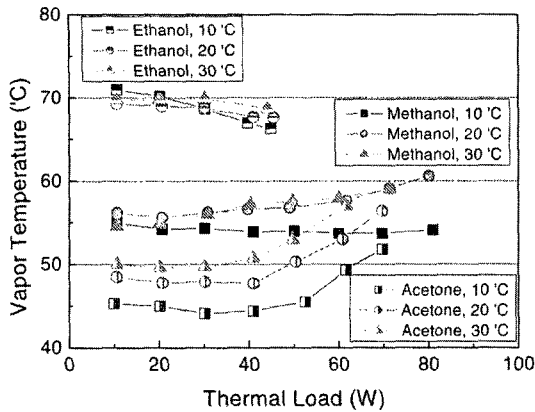


Fig. 5  $Q_{max}$  and  $R_{th}$  for working fluid charge ratio (methanol-1.0 μm LHP for  $T_{cool,in}=20^{\circ}C$ )

represented by increase in  $Q_{max}$  and decrease in  $R_{th}$ .

Figure 5 represents the effect of the working fluid charge ratio ( $\phi$ ) on the maximum thermal load and thermal resistance for methanol-1.0 μm LHP and the coolant temperature of 20°C. For  $\phi=0.1$ , the maximum thermal load was 67 W and the thermal resistance was 1.0 K/W. As working fluid charge ratio was increased, the thermal performance was improved up to  $\phi=0.4$ , then decreased for higher  $\phi$  values. The best thermal performance was exhibited at  $\phi=0.4$  where  $Q_{max}$  was 75 W and the thermal resistance was 0.9 K/W. The thermal resistance did not change much from  $\phi=0.1$  to 0.7.

Figure 6 shows the vapor temperature ( $T_{v,e}$ ) variation of LHP for three different working fluids which exhibited normal operation. The 0.5 μm LHP was tested for three different working fluids for coolant temperatures ( $T_{cool,in}$ ) of 10, 20, and 30°C while the working fluid charge ratio was maintained  $\phi=0.5$  for convenience of the experiment. The minimum thermal load to ensure a normal start-up of the LHP was found to be 10 W or larger.  $T_{v,e}$  variation of the methanol LHP for  $T_{cool,in}=30^{\circ}C$  was almost same as the case for  $T_{cool,in}=20^{\circ}C$  and  $T_{v,e}$  increased slowly as the thermal load increased. For the case of  $T_{cool,in}=10^{\circ}C$ , however,  $T_{v,e}$  slightly decreased as the thermal load increased. For the case of ethanol,  $T_{v,e}$  decreased as the thermal load increased regardless of the cooling temperature. For



**Fig. 6** Vapor temperature ( $T_{v,e}$ ) variation of the  $0.5 \mu\text{m}$  LHP for different heat sink temperatures

the case of acetone,  $T_{v,e}$  was kept almost constant up to the thermal load of 40 W, and then the temperature was increased linearly as the thermal load increased regardless of the cooling temperature. Change of  $T_{v,e}$  by cooling temperature was largest for acetone among the workable working fluids. The  $T_{v,e}$  of LHP was highest for ethanol in general and the value was about 70°C. Methanol LHP operated at 15°C lower temperature than that of ethanol. For any given thermal load, acetone LHP operated at the lowest vapor temperature.

The observation depicted in Fig. 6 can be explained by introducing a criterion for LHP proposed by Gerasimov et al. (1984) and denoted by  $G$  in the following.

$$G = \frac{dP/dT}{\rho_l g} \Big|_{sat} = \frac{\rho_v h_{fg}}{\rho_l T_{v,e} g} \quad (4)$$

By this criterion, working fluids having larger  $dP/dT|_{sat}$  are preferred. For those working fluids  $T_{v,e}$  can be kept lower at the same operating condition. The fact that vapor pressure as well as  $dP/dT|_{sat}$  value of acetone was the largest among the considered working fluids resulted in the lowest  $T_{v,e}$  as appeared in Fig. 6. Based on the relevant properties at 50°C,  $dP/dT|_{sat}$  values of methanol and ethanol correspond to 87% and 46% of that of acetone. It was presumed that these property values resulted in operating vapor temperatures higher than acetone. The reverse

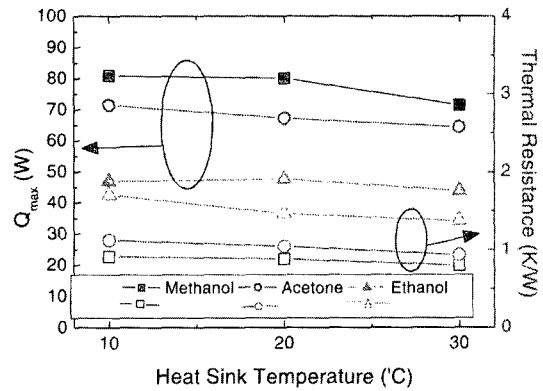


**Fig. 7**  $Q_{\max}$  and  $R_{th}$  of the  $0.5 \mu\text{m}$  LHP for different heat sink temperature

trend of  $T_{v,e}$  for ethanol at low thermal load was considered to have resulted from its poor fluid properties and the insufficient capillary pressure near the operating temperature around 70°C.

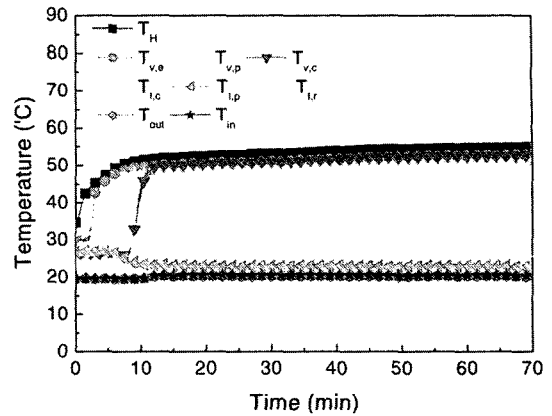
Figure 7 summarizes variation of the maximum thermal load and the thermal resistance of  $0.5 \mu\text{m}$  LHP as a function of coolant inlet temperature for three workable working fluids. Generally, as heat sink temperature increased, the vapor temperature increased as shown in Fig. 6, however, the maximum thermal load and the thermal resistance slightly decreased for any workable working fluid as shown in Fig. 7. The vapor temperature ( $T_{v,e}$ ) of the acetone LHP was the lowest (see Fig. 6) although the thermal performance was not the best (see Fig. 7). The maximum thermal load ( $Q_{\max}$ ) was the highest and the thermal resistance was the lowest for the methanol LHP. The  $Q_{\max}$  of the methanol LHP was 20% higher than acetone LHP and 80% higher than ethanol LHP, and the thermal resistance of the methanol LHP was 20% lower than the acetone LHP and 50% lower than the ethanol LHP. Methanol was considered the best among the workable working fluids in this study. It was expected that the heat transfer rate would be increasing as the temperature difference between heat source and sink increased. The fact that the experimental observation did not match with this expectation can be reasoned as follows. For lower  $T_{cool,in}$ , decreased  $T_{v,e}$  would have worked fa-

vorably for higher  $Q_{\max}$ , which was determined by limiting heater temperature. At the same time however, decreased vapor pressure would have reduced driving force for working fluid circulation and tend to lower  $Q_{\max}$ . For higher  $T_{\text{cool},\text{in}}$ , on the other hand,  $Q_{\max}$  would have tended to decrease due to reduced system temperature difference and limited heater temperature. However, increased system vapor pressure would have enhanced working fluid circulation for higher  $Q_{\max}$ . It is presumed, therefore, that the variation of  $Q_{\max}$  with  $T_{\text{cool},\text{in}}$  was not noticeable as shown in Fig. 7 since the counter effects of the factors associated with heat sink temperature variation were nearly balanced with each other.

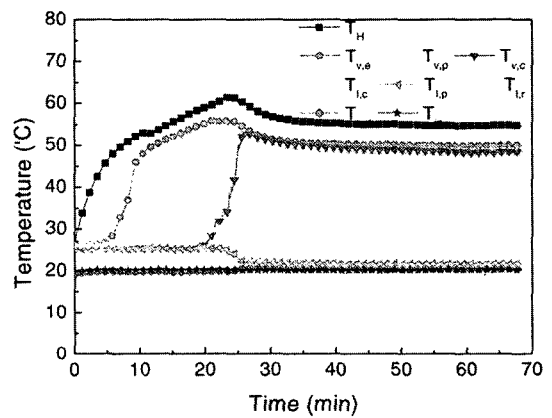
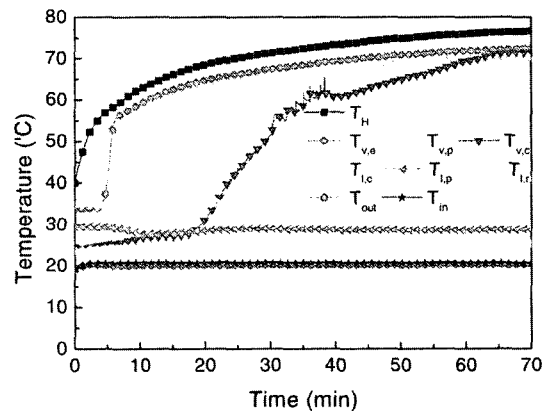
Figure 8 shows the startup characteristics for the coolant temperature of  $20^\circ\text{C}$ . Experiment was conducted to investigate the gravity effect on the methanol- $0.5\ \mu\text{m}$  LHP for  $\phi=0.5$ . For bottom heating mode, the evaporator was located 10 cm below the condenser and for top heating mode, it was located 5 cm above the condenser. For horizontal position (Fig. 8(a)), the temperature of vapor at evaporator outlet ( $T_{v,e}$ ), the middle of the vapor transport line ( $T_{v,p}$ ), and the vapor at the condenser inlet ( $T_{v,c}$ ) were heated up sequentially when the minimum thermal load of 10 W was applied. The LHP reached steady state after 15 min at this condition.

The startup characteristic of the LHP for bottom heating mode (Fig. 8(b)) was similar to thermo syphon. An overshoot was observed between 12 to 25 min and the time to reach the steady-state was delayed by 20 min from the case for horizontal condition. For top heating mode (Fig. 8(c)), it took more than 60 min to reach the steady-state. Although the  $T_{v,c}$  for horizontal position and bottom heating mode was heated up rapidly at certain moment,  $T_{v,c}$  for top heating mode was heated up slowly.

Figure 9 shows the vapor temperature ( $T_{v,e}$ ) variation of the methanol- $0.5\ \mu\text{m}$  LHP for gravity effect. For bottom heating mode ( $-10\ \text{cm}$ ), the maximum thermal load was 95 W and the  $T_{v,e}$  exhibited the lowest values, which linearly increased as thermal load increased. The  $T_{v,e}$  for



(a) Horizontal position

(b) Bottom heating mode ( $-10\ \text{cm}$ )(c) Top heating mode ( $+5\ \text{cm}$ )

**Fig. 8** Startup characteristics of methanol- $0.5\ \mu\text{m}$  LHP at thermal load of 10 W for  $\phi=0.5$  and  $T_{\text{cool},\text{in}}=20^\circ\text{C}$

the top heating mode was the highest, which decreased as thermal load increased until the

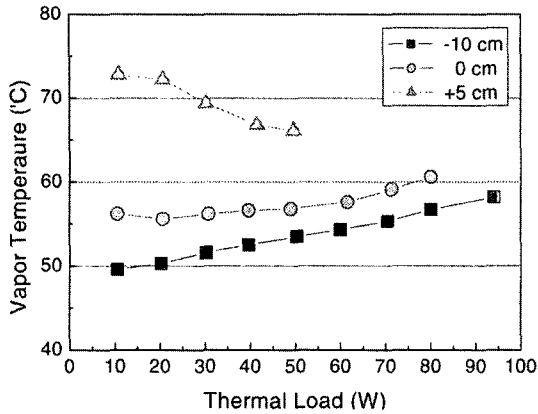


Fig. 9 The vapor temperature ( $T_{v,e}$ ) variation of the methanol-0.5  $\mu\text{m}$  LHP for gravity effect

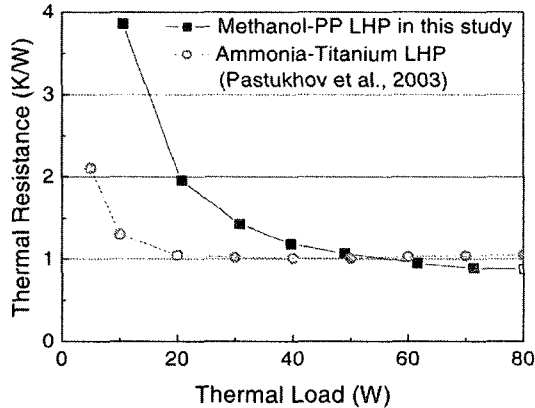


Fig. 10 Thermal resistance comparison of methanol-PP LHP in this study and ammonia-titanium LHP (Pastukhov et al., 2003)

maximum thermal load of 50 W.

Figure 10 compares the thermal resistance of methanol-0.5  $\mu\text{m}$  PP LHP for  $\phi=0.5$  in this study with that of ammonia-titanium LHP having cylindrical evaporator which was reported in Pastukhov et al. (2003). For both LHPs, the thermal load was 80 W while the condenser cooling temperature was 20°C and the inclination angle was 0° (horizontal). The only difference was that Pastukhov et al.'s LHP had a plane heating area of 25 mm by 25 mm on a saddle which was attached to cylindrical evaporator. Although the methanol-PP LHP exhibited higher thermal resistance for thermal loads lower than 40 W, it showed comparable (about 1 K/W), or even

lower, thermal resistances for thermal loads between 50 and 80 W.

#### 4. Conclusions

The thermal performance of a small-scale loop heat pipe with polypropylene (PP) wick was investigated from the view points of pore size of capillary structure, working fluids and their charge ratios, and condenser temperature. Thermal performance was evaluated by the maximum thermal load and the thermal resistance.

Methanol, acetone, and ethanol were used as working fluids of the LHP. Based on the maximum thermal load and the thermal resistance, methanol was considered the best among the workable working fluids in this study. The maximum thermal load for the methanol-0.5  $\mu\text{m}$  LHP was 80 W (6.5 W/m<sup>2</sup>) and the thermal resistance was 0.8 K/W. As pore size reduced from 25  $\mu\text{m}$  to 0.5  $\mu\text{m}$ , the maximum thermal load was increased by 45%. At the same time, thermal resistance of the system was decreased by 33%.

The best thermal performance was exhibited at the working fluid charge ratio was  $\phi=0.4$ , however the thermal resistance did not change much from  $\phi=0.1$  to 0.7.

For top heating mode, time to reach the steady-state was more than 4 times longer than that for horizontal position and the maximum thermal load was 38% less than that for horizontal position.

The LHP developed in this study was able to transport thermal load of 80 W at horizontal position, while maintaining the vapor temperature (i.e., operating temperature) less than 80°C.

#### References

Bazzo, E., Nogoseke, M. and Heinen, L., 2002, "Thermal Behavior of Capillary Pumping Systems Applied to Solar Collectors," *Proceedings of The 12th International Heat Pipe Conference*, Moscow, Russia, pp. 514~518.

Bienert, W. B., Krotiuk, W. J. and Nikitkin, M. N., 1999, "Thermal Control With Low-Power, Miniature Loop Heat Pipes," *SAE Transac-*



- tions — Section 1, *Journal of Aerospace*, SAE No. 1999-01-2008, pp. 520~524.
- Boo, J. H., Yoon, C. and Peterson, G. P., 1995, "Experimental Study on the Thermal Performance of a Capillary Pumped Loop Having a Flat Evaporator," *The ASME/AIAA National Heat Transfer Conference*, Portland, Oregon, USA, AIAA Paper No. 95-3514.
- Boo, J. H., 2000, "Effect of Mesh Size in a Flat Evaporator and Condenser Cooling Capacity on the Thermal Performance of a Capillary Pumped Loop," *KSME International Journal*, Vol. 14, No. 1, pp. 121~129.
- Delil, A. A. M., Baturkin, V., Friedrichson, Yu., Khmelev, Yu. and Zhuk, S., 2002, "Experimental Results of Heat Transfer Phenomena in a Miniature Loop Heat Pipe with a Flat Evaporator," *Proceedings of The 12th International Heat Pipe Conference*, Moscow, Russia, pp. 126~133.
- Gerasimov, Yu. F. Maidanik, Yu. F., Dolgirev, Yu. F. and Kiseev, V. M., 1984, "Antigravitational Heat Pipes - Development, Experimental and Analytical Investigation," *Proceedings of The 5th International Heat Pipe Conference*, Tsukuba, Japan, pp. 82~88
- Goncharov, K. A., Nikitkin, M. N., Golovin, O. A., Fershtater, Yu. G., Maidanik, Yu. F. and Piukov, S. A., 1995, "Loop Heat Pipe in Thermal Control Systems for "OBZOR" Spacecraft," *The 25th International Conference on Environmental Systems*, California, USA, SAE No. 951555.
- Hoang, T. T. and Ku, J., 2002, "Advanced Loop Heat Pipes for Spacecraft Thermal Control," *Proceedings of The 8th AIAA/ASME Joint Thermophysics and Heat Transfer Conference*, Missouri, USA, AIAA 2002-3094.
- Ishikawa, H., Yao, A., Ogushi, T., Haga, S., Miyasaka, A. and Noda, H., 2001, "Development of Loop Heat Pipe Deployable Radiator for Use on Engineering Test Satellite VIII (ETS-VIII)," *SAE Transactions - Section 1, Journal of Aerospace*, SAE No. 2001-01-2341, pp. 115~121.
- Kiseev, V.M., Maidanik, Yu.F. and Gerasimov, Yu. F., 1984, "Heat-Transporting Device," *United States Patent*, No. 4,467,861.
- Kobayashi, T., Ogushi, T., Haga, S., Ozaki, E. and Fujii, M., 2003, "Heat Transfer Performance of a Flexible Looped Heat Pipe Using R134a as a Working Fluid: Proposal for a Method to Predict the Maximum Heat Transfer Rate of FLHP," *Heat Transfer-Asian Research*, Vol. 32, No. 4, pp. 306~318.
- Kozmine, D., Goncharov, K., Nikitkin, M., Maidanik, Yu. P., Fershtater, Yu. G. and Fiodor, S., 1996, "Loop Heat Pipes for Space Mission Mars 96," *The 26th International Conference on Environmental Systems*, California, USA, SAE No. 961602.
- Lee, W. H., Lee, K. W., Park, K. H., Lee, K. J. and Noh, S. Y., 2004, "Study on a Operating Characteristics of Loop Heat Pipe Using a Brass Sintered Metal Wick-Water," *Proceedings of The KSME 2004 Spring Annual Meeting in Korea*, pp. 1528~1533.
- Maidanik, Yu. F., Vershinin, S. V., Kholodov, V. F. and Dolgirev, Yu. E., 1985, "Heat Transfer Apparatus," *United States Patent*, No. 4,515,209.
- Maidanik, Yu. F., Fershtater, Yu. G. and Solodovnik, N. N., 1994, "Loop Heat Pipes: Design, Investigation, Prospects of Use in Aerospace Technics," *SAE Aerospace Atlantic Conference*, Ohio, USA, Paper No. 941185.
- Maidanik, Yu. F., 1999, "State-of-the-art of CPL and LHP Technology," *Proceedings of The 11th International Heat Pipe Conference*, Tokyo, Japan, K-II, pp. 19~30.
- Pastukhov, V. G., Maidanik, Yu. F. and Chernyshova, M. A., 1999, "Development and Investigation of Miniature Loop Heat Pipes," *SAE Transactions — Section 1, Journal of Aerospace*, SAE No. 1999-01-1983, pp. 483~487.
- Pastukhov, V. G., Maidanik, Yu. F., Vershinin, C. V. and Korukov, M. A., 2003, "Miniature loop heat pipes for electronics cooling," *Applied Thermal Engineering*, Vol. 23, Issue 9, pp. 1125~1135.
- Schlitt, R., Dubois, M., Ounougha, L. and Supper, W., 2000, "COM2PLEX — a Combined European LHP Experiment on SPACEHAB/QUEST," *The 30th International Conference on Environmental Systems*, Toulouse, France, SAE No. 2000-01-2457.
- Swanson, T. D. and Birur, G. C., 2003, "NASA

Thermal Control Technologies for Robotic Spacecraft," *Applied Thermal Engineering*, Vol. 23, Issue 9, pp. 1055~1065.

Waterman, N. A. and Ashby, M. F., 1997, *The Materials Selector*, Vol. 3, 2nd ed., Chapman & Hall, London, pp. 42~109.